

Phase segregation of polymerizable lipids to construct filters for separating lipid-membrane-embedded species

Shu-Kai Hu, Ya-Ming Chen, and Ling Chao^{a)}

Department of Chemical Engineering, National Taiwan University, No. 1, Sec. 4, Roosevelt Road, Taipei 10617, Taiwan

(Received 30 May 2014; accepted 2 September 2014; published online 12 September 2014)

Supported lipid bilayer (SLB) platforms have been developed to transport and separate membrane-embedded species in the species' native bilayer environment. In this study, we used the phase segregation phenomenon of lipid mixtures containing a polymerizable diacetylene phospholipid, 1,2-bis(10,12-tricosadiynoyl)-sn-glycero-3-phosphocholine (DiynePC), and a nonpolymerizable phospholipid, 1,2-dioleoyl-sn-glycero-3-phosphocholine (DOPC), to create filter barrier structures in SLBs. Upon exposing the phase segregated samples to UV light, the DiynePC-rich domains could become crosslinked and remain fixed on the surface of the support, while the DOPC-rich regions, where no crosslinking could happen, could be removed later by detergent washing, and thus became the void regions in the filter. During the filter fabrication process, we used the laminar flow configuration in a microfluidic channel to control the spatial locations of the feed region and filter region in the SLB. The flow in a microfluidic channel was also used to apply a strong hydrodynamic shear stress to the SLB to transport the membrane-embedded species from the feed region to the filter region. We varied the DiynePC/DOPC molar ratio from 60/40 to 80/20 to adjust the cutoff size of the filter barriers and used two model membrane-embedded species of different sizes to examine the filtering capability. One of the model species, Texas Red 1,2-dihexa-decanoyl-sn-glycero-3-phosphoethanolamine triethylammonium salt (Texas Red DHPE), had a single-lipid size, and the other species, cholera toxin subunit B-GM1 complex, had a multilipid size. When the DiynePC/DOPC molar ratio was 60/40, both species had high penetration ratios in the filter region. However, when the ratio was increased to 70/30, only the Texas Red DHPE, which was the smaller of the two model species, could penetrate the filter to a considerable extent. When the ratio was increased to 80/20, neither of the model species could penetrate the filter region. The results showed the possibility of using phase segregation of a mixture containing a polymerizable lipid and a nonpolymerizable lipid to fabricate filter barrier structures with tunable cutoff sizes in SLBs. © 2014 AIP Publishing LLC.

[<http://dx.doi.org/10.1063/1.4895570>]

INTRODUCTION

Understanding the functions and structures of cell-membrane-associated species could help estimate how a certain signal or pathogen can enter a cell.^{1,2} However, most cell membrane species have structures adapted to the cell membrane's lipid bilayer, which is amphiphilic in nature, leading to difficulties in maintaining their functions after they are removed from cell membranes for further characterization. Current strategies rely on the use of amphiphilic chemicals to purify membrane species derived from cell membranes.^{3,4} These approaches may cause denaturation of the membrane species, or disrupt the species' functions associated with interactions with the surrounding lipid bilayer. Consequently, approaches that can process and

^{a)}E-mail: lingchao@ntu.edu.tw

characterize membrane species in native-like environments could significantly increase our understanding about the functions of various cell membrane species.

Recent studies have attempted to separate and characterize membrane-embedded species in supported lipid bilayers (SLBs) to protect the species' delicate hydrophobic core in a native lipid bilayer environment.⁵⁻⁷ SLBs are planar extended bilayers adsorbed on a suitable solid surface,^{8,9} and they have lateral fluidity.¹⁰⁻¹² Several methods with different driving forces have been reported to transport membrane species in SLBs, including electrophoresis,¹³ electrophoretic-electroosmotic focusing,¹⁴ hydrodynamic force,¹⁵ and surface acoustic waves.¹⁶ However, current approaches focus on investigating different types of driving forces, and few approaches have been developed to modulate the properties of the lipid bilayer separation medium.^{6,13,17}

Based on the concept that conventional separation processes such as filtration and chromatography can be made more effective by adding barriers to the separation medium,¹⁸ we attempted to create solid barriers in two-dimensional SLBs. Membrane species responding differently to the barriers can therefore be separated. We used a polymerizable lipid, 1,2-bis(10,12-tricosadiynoyl)-sn-glycero-3-phosphocholine (DiynePC), to construct solid barriers.^{17,19} The DiynePC lipid has triple bonds, and it can covalently bond with a neighboring DiynePC lipid in the bilayer structure after being exposed to 254 nm UV light.²⁰ In our previous study, we showed that UV irradiation can be used to control the degree of cross-linking of DiynePC SLBs, resulting in the formation of a solid matrix with pores. However, several studies have shown that the cross-linked regions are distributed randomly and cross-linked regions in the two leaflets of the bilayers may not coincide,^{17,19,20} which leads to difficulties in constructing clean continuous paths larger than nanometer size in the matrix. In particular, cross-linking occurs in the 2D planar membrane, and the pore size indicates the pore surface area in the 2D planar membrane platform. The aforementioned random property limits the use of the platform to the separation of extremely small transmembrane species. In addition, noncoincident cross-linking could cause some hydrophobic DiynePC acyl chains to be exposed to the external aqueous environment, leading to nonspecific binding problems. To increase SLB applications, it is desirable to develop an alternative method to construct barrier structures with larger voids, clean paths, and sizes that are more suitable for typical transmembrane proteins.

In this study, we used the phase-segregation phenomenon of lipid mixtures containing both polymerizable DiynePC and non-polymerizable 1,2-dioleoyl-sn-glycero-3-phosphocholine (DOPC) to construct filter barrier structures in SLBs. DiynePC has been observed to phase-segregate when mixed with several other commonly used saturated and unsaturated lipids. After phase segregation, the samples were exposed to UV light to cross-link DiynePC-rich phase domains to form solid filter matrices; the nonpolymerizable lipids were washed away, leaving void regions. In the fabrication process, we used the laminar flow configuration in the microfluidic channel to control the spatial locations of the feed region and the filter region in the SLB. Because the phase-segregated domains in the upper and lower leaflets of the bilayers coincide,²¹ and according to nucleation theory, the stable-phase-segregated domain size should be larger than a critical size²² and the constructed filter's void region should be clear and larger than the size of few lipid molecules. We varied the DiynePC/DOPC molar ratio from 60/40 to 80/20 to adjust the cutoff size of the filter barrier and used two model membrane-embedded species in the typical size range of transmembrane proteins and lipids to examine the filtering capability of the constructed SLB platforms.

EXPERIMENTAL

Materials

Diacetylene phospholipid (DiynePC), 1,2-dioleoyl-sn-glycero-3-phosphocholine (DOPC), and the bovine brain ganglioside GM1 were purchased from Avanti Polar Lipids (Alabaster, AL). Texas Red 1,2-dihexa-decanoyl-sn-glycero-3-phosphoethanolamine triethylammonium salt (Texas Red DHPE) and Alexa Fluor[®] 488 conjugated cholera toxin subunit B were purchased from Invitrogen (Eugene, OR). Polydimethylsiloxane (PDMS; Sylgard 184) used to fabricate microfluidic channels was purchased from Corning (Corning, NY). Sodium dodecyl sulfate (SDS) was purchased from Sigma (St. Louis, MO).

Preparation of large unilamellar vesicles for lipid vesicle deposition

A vesicle deposition method was used to form SLBs on glass supports.¹³ Different weight percentages of DiynePC and DOPC (60/40, 70/30, or 80/20) were mixed together in chloroform with 0.5 mol. % of Texas Red DHPE or 1 mol. % of bovine brain ganglioside GM1. The chloroform was then removed under vacuum. The dried lipids were then reconstituted in phosphate-buffered saline (PBS) buffer (10 mM phosphate and 150 mM NaCl at a pH of 6.6) with a concentration of 0.2 mg/ml. The lipid mixture solution was heated to 50 °C and then passed 19 times through a 50 nm polycarbonate filter in an Avanti Mini-Extruder (Alabaster, AL) to form large unilamellar vesicles (LUVs). The prepared LUV solutions were kept at 50 °C and sent into a microfluidic device that had been heated to the same temperature. The LUV solutions were in contact with the desired region for 5 min and rinsed extensively with buffer at the same temperature. After the vesicle deposition process, the sample was placed in a water bath that was cooled from 50 °C to 15 °C in 1.5 h at a constant rate. The temperature was controlled and monitored using an immersion circulator (model PC200, Thermo Fisher Scientific, Waltham, MA).

Preparation of supported lipid bilayers in a microfluidic device

The cross-shaped microfluidic channel (each arm is 460 μm wide and 110 μm high) was made of PDMS using the soft lithography technique. The mold for PDMS casting was fabricated using SU8 photoresist (Microchem, USA). Glass coverslips were cleaned with argon plasma for 10 min and treated with oxygen plasma for 30 s before being used for sealing to a PDMS microchannel slab. When the lipid vesicle deposition method was used to form SLBs in a microchannel, the vesicles were exposed to the glass surface for 5 min under the flow and then rinsed with buffer for 5 min every time a lipid membrane was formed. During the SLB formation, the flow rates of the lipid vesicle solutions and rinsing buffer were maintained at 80 $\mu\text{l}/\text{min}$ in all arms of the device.

After the desired SLBs were formed in the microchannel, they were irradiated with light from a UV lamp (UVP, 254 nm) for 2 h at room temperature. The sample was placed at a distance of 1 cm from the lamp, and the UV intensity was around 0.6 mW/cm² at 254 nm. After UV irradiation, non-cross-linked DiynePC monomers and DOPC were removed from the substrate surface by passing 0.1 M SDS solution through the microchannel at 30 °C and allowing it to sit for 30 min. Later, deionized water was flowed into the channel to rinse the sample thoroughly. The cross-linked DiynePC membranes were stored in the dark at 4 °C before use.

Fluorescence microscopy and image processing to calculate the cross-linked/void area ratio

Fluorescence images were obtained using an Olympus IX81 inverted microscope and a CCD camera (ORCA-R2, Hamamatsu, Japan). Fluorescence from Alexa-Fluoro 488[®] fluorophore and Texas Red fluorophore was observed using the Olympus U-WIBA filter set (excitation wavelength: 470–490 nm; emission wavelength: 510–550 nm) and the U-DM-CY3–3 filter set (excitation wavelength: 510–550 nm; emission wavelength: 570–620 nm), respectively. The area fraction of the dark region in the fluorescence images was calculated with Matlab software (MathWorks Inc., Natick, MA). The defined dark region was delineated using an image processing routine that can eliminate uneven background in the case of uneven illumination and define the dark region by using Otsu's threshold method.²³

RESULTS AND DISCUSSION

Principle of the method

We used phase segregation in the DiynePC/DOPC SLB to construct filters for membrane-embedded species. DiynePC has triple bonds on both acyl chains, and several studies have shown that they tend to align together and form domains in mixtures with other commonly used lipids.^{24,25} In this study, we used DOPC to induce lipid membrane phase segregation

because DOPC has a transition temperature of -17°C and tends to be in its disordered fluid state at room temperature. The transition temperature of DiynePC is 38°C , and it tends to be in an ordered state at room temperature; therefore, phase segregation of the mixture is possible at room temperature. After phase segregation and exposure to UV light, only domains rich in DiynePC can be cross-linked to form solid filter barriers; the regions rich in nonpolymerizable DOPC are transformed to void regions in the filter.

As illustrated in Figure 1, we used the DiynePC/DOPC molar ratio to control the phase segregation pattern and thus, the cutoff size of the filter. The larger the DiynePC/DOPC molar ratio, the larger will be the area of the DiynePC-rich domains and the smaller will be the area of the void regions. When the membrane species embedded in the SLB were forced to pass through the filter area, only the species with sizes smaller than the void path could pass through. We used the hydrodynamic force of the bulk flow in the microchannel to transport the embedded biomolecules from the feed region to the cross-linked region in the lipid membrane, similar to one of our earlier studies.¹⁷ Because of the small length of the microchannel, a high flow rate can be easily maintained; the high flow rate leads to a large shear stress being applied to the SLB. In principle, the large shear stress can move the fluid SLB relative to the solid support;²⁶ however, in practice, the cross-linked DiynePC matrix cannot be easily moved by the bulk flow shear stress and can be viewed as a stationary barrier.¹⁷

Using a microfluidic device to fabricate a filter in a lipid membrane platform

To control the spatial locations of both the filter and the feed region in a membrane platform, we used laminar flow in the microfluidic channel. We used the lipid vesicle deposition method to form SLBs, and the SLBs formed only on the surface where the vesicles were in contact. In a microchannel, the directions of vesicle streams can be accurately controlled and

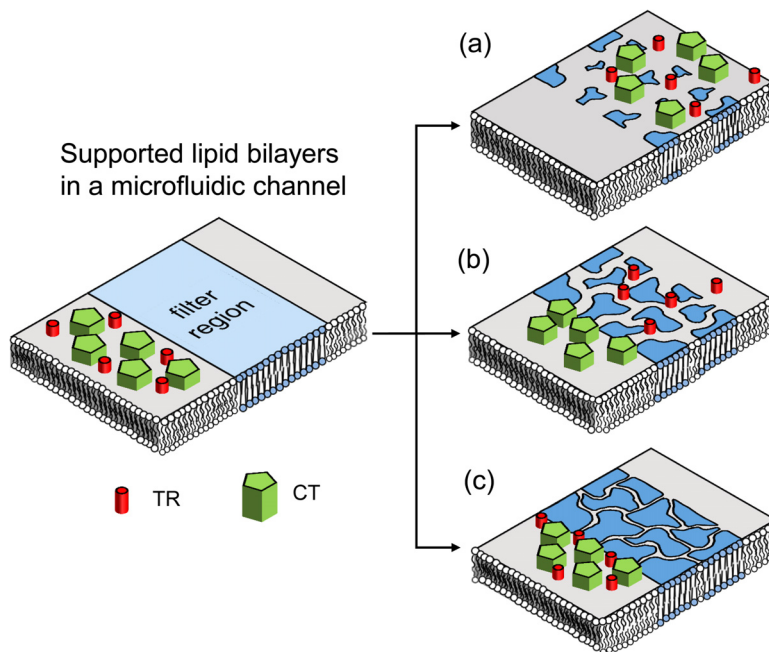


FIG. 1. Illustration of a filter used to separate membrane-embedded species in the SLB. After phase segregation, the DiynePC-rich phase domains can be cross-linked to form barriers (dark blue region). The membrane species can be transported in the fluid non-cross-linked lipid bilayer region. When the membrane species embedded in the SLB were forced to pass through the filter region, only the species with sizes smaller than the void region size can penetrate the filter area. In this study, we used two model species embedded in the membrane, Texas Red DHPE (TR, red object) and cholera toxin subunit B-GM1 complex (CT complex, green object), to demonstrate the filtering capability. (a) When the area ratio of the DiynePC-rich phase to the DOPC-rich phase is low, both the species can penetrate the filter region. (b) When the ratio increases and the pore size decreases, only the smaller species can penetrate to a considerable extent. (c) When the ratio further increases, both the species can no longer penetrate.

the lipid vesicles can be deposited to form SLBs in the desired regions. Once the SLBs were formed, a strong hydrodynamic shear stress was provided by the bulk flow in the microchannel to transport the membrane species in the membrane platform.

Figure 2 illustrates the procedure that we used to form the filter membrane platforms in the cross-shaped microchannel. First, we introduced the DiynePC/DOPC lipid vesicles from the right channel and a buffer stream from the left channel and let them leave through the top and bottom channels. The buffer stream was used to confine the formation of the DiynePC/DOPC lipid membrane (light blue color) to the right half of the channel (Figure 2(a)). Before and in the first step, the entire system was heated to 50 °C, and therefore, the DiynePC/DOPC lipid vesicles readily fused with the glass surface and remained as a homogeneous SLB without phase segregation. Subsequently, a 50 °C buffer was used to wash away the excess vesicles. Phase segregation was induced by decreasing the sample temperature from 50 °C to 15 °C at a cooling rate of 23 °C/h (Figure 2(b)). In all experiments, the slow and controlled cooling allowed the different phase domains to reach equilibrium, resulting in the segregation phase ratio and pattern becoming stable. After phase segregation, the SLBs formed were provided an overdose of UV light to ensure that all the DiynePC-rich phase domains were fully cross-linked and the non-cross-linked DiynePC lipids were removed with SDS (Figure 2(c)). The subsequent rinsing steps followed the procedure presented in our previous paper.¹⁷ Next, as illustrated in Figure 2(d), the feed vesicles were introduced from the left channel and the fresh DOPC vesicles were input from the right channel. Two types of feed vesicles were used: One contained 0.5 mol. % TR in DOPC, and the other contained 1 mol. % GM1 in DOPC; GM1 could form complexes with CT after vesicle deposition. Both streams were forced to exit through the top and bottom channels to ensure that the feed vesicles remained on the left side of the channel and the fresh DOPC vesicles were confined to the right side. The DOPC vesicles can only refill empty glass surfaces where cross-linked DiynePC lipids are absent. The reason for removing the non-cross-linked DOPC membrane in the DiynePC matrix and refilling fresh DOPC in the matrix is that the DOPC has two unsaturated acyl chains and could easily denature upon prolonged exposure to UV. The DOPC membrane and feed membrane were highly fluidic and could be considered as a solution phase in the SLB. After the feed region and filter region were formed, the top and bottom channels were blocked, and buffer solutions were sent from the left channel to the right channel at a flow rate of 400 $\mu\text{L}/\text{min}$ to transfer the model membrane species from the feed region to the filter region (Figure 2(e)).

Phase segregation in DiynePC/DOPC SLBs

We prepared SLBs with different DiynePC/DOPC molar ratios. To obtain the phase segregation morphology, we added 0.5 mol. % of TR to the DiynePC/DOPC mixture for partitioning the mixture and forming a DOPC-rich phase; the difference in the fluorescence intensity between the two phases could be used to distinguish the phase boundaries. The images on the right side in Figure 3 show the phase segregation morphology in the SLBs for DiynePC/DOPC molar ratios of 80/20, 70/30, and 60/40. The area of the DiynePC-rich phase region (dark

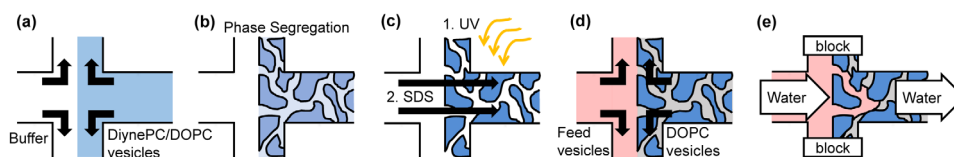


FIG. 2. Illustration of the procedure used to form a filter membrane platform in a cross-shaped microchannel. The channel had four arms, and each arm was 0.7 cm long, 460 μm wide, and 110 μm high. Laminar flow was used to pattern the different regions in the SLB platform. (a) Formation of a homogeneous DiynePC/DOPC (light blue) SLB on the right side of the channel. (b) Decreasing the sample temperature to induce phase segregation: DiynePC-rich phase (darker blue) and DOPC-rich phase (lighter blue). (c) Exposure to UV light for cross-linking the DiynePC-rich phase region (dark blue) and performing SDS wash to remove the non-cross-linked region. (d) Formation of the feed membrane and refilling with fresh DOPC lipids to form the fluid region in the filter matrix. (e) Transporting the model membrane-embedded species in the feed region (pink) to the filter region by using the flow in the microfluidic channel.

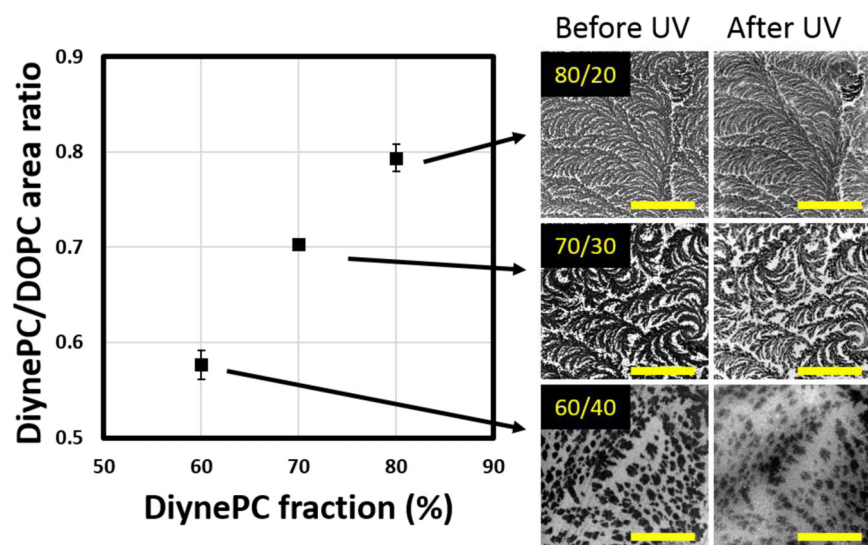


FIG. 3. Phase segregation morphology images and area ratios in the SLBs with DiynePC/DOPC molar ratios of 80/20, 70/30, and 60/40. The “Before UV” images were taken after phase segregation of the DiynePC/DOPC membranes. The membranes contained 0.5 mol. % of TR, which helped in identifying the two phases. The “After UV” images were taken after UV exposure, removal of the non-cross-linked DOPC, and refilling of fresh DOPC containing 0.5 mol. % of TR. The scale bar length is 100 μm . Data are represented as means with standard deviation ($n = 3$).

region) decreased and that of the DOPC-rich region (bright region) increased when the DiynePC/DOPC molar ratio decreased from 80/20 to 60/40. We further performed image processing to calculate the area ratios after phase segregation and found that they were similar to the DiynePC/DOPC molar ratios in the SLBs (left diagram in Figure 3), suggesting that the compositions of the two phases could be close to those pure DiynePC and pure DOPC. We observed that the membrane morphologies after exposure to UV light, removal of non-cross-linked lipids, and refilling of fresh DOPC (“After UV” images in Figure 3) were very similar to those observed immediately after phase segregation before UV exposure (“Before UV” images in Figure 3), suggesting that most of the DiynePC-rich domains were highly cross-linked following UV irradiation.

Filtering model membrane species in SLBs

To demonstrate the functioning of the filter in the membrane platform, we chose two model membrane species with different sizes of their membrane-embedded parts, as shown in Figure 4(a). One of the species was TR, which is a phospholipid with a Texas Red fluorophore attached to the head group and which has a membrane-embedded size similar to that of a regular phospholipid. If we view TR as a cylinder embedded in the membrane, the equivalent diameter is about 0.9 nm,²⁷ as illustrated in Figure 4(a). The other model species was the Alexa Fluor[®] 488-conjugated CT complex. Cholera toxin subunit B is a pentamer and can capture up to five GM1 lipids in the lipid membrane. If the five binding sites of cholera toxin subunit B are all occupied by GM1 lipids and the CT complex is viewed as a cylinder, the equivalent diameter is around 5.4 nm;²⁸ however, one cholera toxin subunit B does not always bind to five GM1 lipids in the membrane and the complex could have one, two, three, four, or five GM1 lipids. In this study, we first used the vesicle deposition method to form the feed membrane with 99 mol. % DOPC and 1 mol. % GM1. Subsequently, we added cholera toxin subunit B solution (2 $\mu\text{g}/\text{ml}$ in PBS buffer) to the feed membrane region to form CT complexes. The concentration conditions required to allow one cholera toxin subunit B to bind to at least three GM1 lipids to form a complex have previously been shown.²⁶ In addition, the movement speed of the complex in our control DOPC experiment (shown in supplementary material²⁹) also matched a previously reported speed of the complex with more than three GM1 lipids.³⁰ As

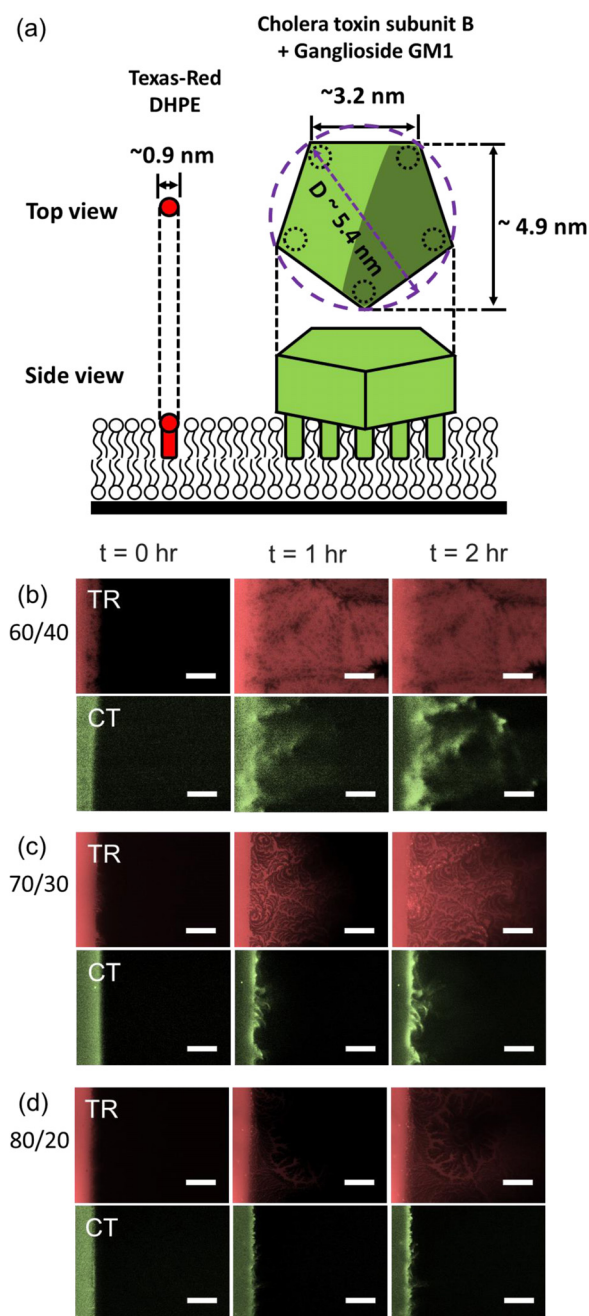


FIG. 4. Penetration of the filter region in the SLBs by the model membrane-embedded species. (a) The two model membrane species used in this study: TR (left side) and CT complex (right side). (b) Both TR and CT complex could penetrate the (60/40) DiynePC/DOPC membrane filter to a considerable extent in 2 h. (c) Only TR could penetrate the (70/30) DiynePC/DOPC membrane filter to a considerable extent in 2 h. (d) Neither TR nor CT-complex could penetrate the filter constructed by the (80/20) DiynePC/DOPC membrane filter in 2 h. The scale bar length is $100 \mu\text{m}$.

illustrated in Figure 4(a), the five binding sites of the regular pentagon-shaped cholera toxin subunit B are located at the corners of the pentagon. If three of the binding sites of one CT are occupied by GM1 lipids in the membrane, the longer side of the membrane-embedded part is still about 5.4 nm in length and the short side is about 1.6 nm, which is several times the size of the membrane-embedded part of TR.

The filter barrier area fraction increased and the void region area decreased when the DiynePC/DOPC molar ratio was increased. We used the shear force provided by the bulk flow

in the microfluidic channel to drive the membrane species toward the filter region.^{15,26} When the ratio was 60/40, both species could penetrate the filter region to a considerable extent. However, when the ratio was increased to 70/30, only the smaller species (TR) could penetrate the filter region. When the ratio was increased to 80/20, the continuous path appeared to become considerably small and neither TR nor CT complex could penetrate the filter region.

Since the initial concentrations of the model species, the shapes and sizes of the model species, and the bulk flow rate can all influence the penetration rate, we further defined a relative penetration ratio to quantitatively compare the filtering capability of the platforms for the two membrane species. The penetration ratios were obtained by dividing the rate of penetration of the species of interest through the designated filter region by the rate of penetration through a control region without any filter barriers (as shown in the pure DOPC control experiment in Supplementary Information²⁹). The penetration rate was obtained by calculating how the overall fluorescence intensity of the target species in the filter region changes with time. Figures 4(b)–4(d) show part of the representative images we used to obtain the penetration rate of the model species in the SLBs with DiynePC/DOPC molar ratios of 60/40, 70/30, and 80/20. The penetration rates of the two species through the control membrane with pure DOPC were obtained from the control experiment images presented in supplementary material.²⁹

Figure 5 shows the penetration ratios of the two model species in the SLBs for DiynePC/DOPC molar ratios of 60/40, 70/30, and 80/20. These penetration ratios were obtained when a surface shear stress close to 7.35 N/m^2 was applied to the membrane. The shear stress was generated by using a bulk flow rate of $400 \mu\text{l/min}$ in the $460 \mu\text{m}$ wide and $110 \mu\text{m}$ high microchannel. The penetration ratios of both species were high when the DiynePC/DOPC molar ratio was 60/40. The penetration ratio of the larger species (CT complex) in a 70/30 DiynePC/DOPC filter dropped considerably from the one in a 60/40 DiynePC/DOPC filter (ANOVA with Tukey's HSD test, $p < 0.05$, $n = 3$). However, the penetration ratio of the smaller species (TR) in a 70/30 DiynePC/DOPC filter did not change significantly from the one in a 60/40 DiynePC/DOPC filter, but the penetration ratio dropped considerably in an 80/20 DiynePC/DOPC filter (ANOVA with Tukey's HSD test, $p < 0.05$, $n = 3$). The penetration ratios of both species were low when we used an 80/20 DiynePC/DOPC filter. These data further suggested that we could use the DiynePC/DOPC molar ratio to adjust the phase segregation pattern and therefore, the filter cutoff size.

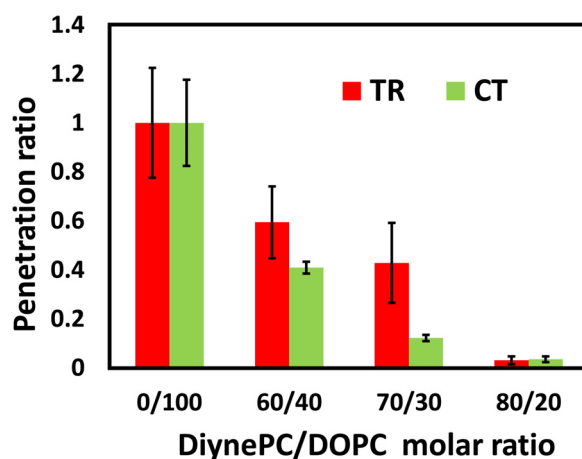


FIG. 5. The penetration ratios of the two model species, TR (red bars) and CT complex (green bars), through the filters constructed by membranes with various DiynePC/DOPC molar ratios. The penetration ratio in the y-axis was obtained by dividing the penetration rate of the species of interest through the designated platform by that through a control region without any filter barrier (pure DOPC or a DiynePC/DOPC molar ratio of 0/100). Data are represented as means with standard deviation. For TR, the penetration ratio in an 80/20 DiynePC/DOPC filter but not a 70/30 DiynePC/DOPC filter has a significant difference from the one in a 60/40 DiynePC/DOPC filter (ANOVA with Tukey's HSD test, $p < 0.05$, $n = 3$). On the other hand, for CT complex, both the penetration ratios in 80/20 and 70/30 DiynePC/DOPC filters are significantly different from the one in a 60/40 DiynePC/DOPC filter (ANOVA with Tukey's HSD test, $p < 0.05$, $n = 3$).

Although a significant amount of TR appeared to penetrate the filter region in the 80/20 DiynePC/DOPC membrane, as shown in Figure 4(d), the penetration ratios of TR and CT complex in the 80/20 membrane were both close to zero, as shown in Figure 5. The reason is that the penetration ratio is the penetration rate normalized by the penetration rate in the pure DOPC control experiment. In the control experiments (details provided in supplementary material²⁹), the penetration rate of TR was larger than that of CT complex when we applied the same bulk flow driving force. Therefore, although the penetration rate of TR appeared to be significant, the normalized ratio was still low. In addition, we used the fluorescence intensity to calculate the penetration rate. In general, the fluorescence intensity is significantly influenced by the intrinsic fluorescence characteristics of the probe used, the camera exposure time, and the environment where the probe is stored. Therefore, the measured fluorescence intensities from two different membrane species cannot be used to compare the amounts of the species. A comparison of the penetration ratios, which were normalized by the penetration rates in the control experiments, can more accurately show the filtering capability of a designated platform to the interested species.

Advantages of using phase segregation to generate the barrier structure

We generated the filter barrier structure by using phase segregation of DiynePC lipids from nonpolymerizable lipids. According to nucleation theory, the smallest feature size generated by the phase-segregation method should be larger than the size of few lipid molecules.^{22,31} During the new phase-nucleation process, the new phase components tended to cluster together to decrease the chemical potential of the system; however, the clustering can cause an unfavorable increase in the interfacial energy. The combination of the chemical potential energy reward and the interface energy penalty results in an energy barrier during the nucleation process. Only when the new phase components attain a critical size through clustering and overcome the energy barrier, the new phase domains can be stable. Therefore, the smallest feature size generated by phase segregation should be larger than the critical size, which is equal to at least the combined size of several lipids.

Compared with the other possible methods for constructing porous barrier structures in SLBs, the phase-segregation method could provide clean paths and a more suitable cutoff size range for typical transmembrane biomolecules (with sizes ranging from few nanometers to tens of nanometers). Previous studies using partial cross-linking of a homogeneous DiynePC^{17,19} could be used to construct a porous barrier structure with a nanometer cutoff size. However, the cross-linking of DiynePC in the upper and lower leaflets of the lipid membrane can be random, and the cross-linked regions may not coincide, which could cause problems, as mentioned in the "INTRODUCTION" section. Another possible method to construct a porous barrier structure is to use a photomask to control the exposure to UV light and therefore control the cross-linked region.^{19,32} However, during photolithography, the smallest feature size is limited by the light diffraction limit; therefore, it is difficult to have a cutoff size smaller than submicron dimensions. The typical membrane-embedded biomolecule sizes are typically much smaller than submicron dimensions, and it would be difficult to use photolithography to construct a barrier with a suitable cutoff size for filtering membrane-embedded biomolecules.

Possibilities to adjust the barrier structure

Three factors may strongly influence the phase segregation morphology. The first factor is the amount of DiynePC in the lipid membrane, the second is the ratio of the DiynePC-rich domain growth rate to the domain nucleation rate, and the third is the ratio of the domain growth rate to the domain material mass transfer rate. The higher the DiynePC ratio, the larger the area of the DiynePC-rich phase. Furthermore, the number of domain nuclei and the domain size are inversely correlated when the overall new phase amount is fixed.²² If the growth rate/nucleation rate is higher, there would be lesser but larger domains, causing a less continuous void region, and vice versa. The growth rate/mass transfer rate could influence the domain shape. The dendritic pattern can form when the domain growth is limited by the mass transfer rate of the

domain materials to the growth sites.²² Increasing the mass transfer rate of DiynePC molecules in the membrane or decreasing the domain growth rate could make the domain shape rounder. In fact, in the 60/40 DiynePC/DOPC membrane, the domains were rounder, probably because the DiynePC concentration was smaller, which makes the growth rate lower.

In this study, we prepared the filter membrane in its homogeneous state and gradually cooled the system below the phase transition temperature to induce phase segregation. The formation of new phase nuclei is known to be a kinetic process,^{22,31} and it could be significantly influenced by the cooling rate, the chemical potential difference between the new state and the original homogeneous state, and the interfacial energy between the coexistent phases formed. When the cooling rate is higher, there could be more nuclei and smaller domain and pore sizes, leading to a barrier structure with a smaller cutoff size. When the cooling rate is lower, there should be less nuclei but larger domain and pore sizes, leading to a barrier structure with a larger cutoff size. In addition, although DOPC was mixed with DiynePC as the segregating lipid in this study, other lipids, such as DPPC and POPC, could be also used for this purpose,^{24,25} and based on their incompatibility with DiynePC, the nucleation rate could be tuned and used to generate different phase-segregated morphologies.

CONCLUSION

We successfully used a microfluidic device to construct filters in SLB platforms for separating two model membrane-embedded species. The barrier structure of the filters was constructed through phase segregation of mixtures of polymerizable DiynePC and nonpolymerizable DOPC. Exposure of the phase-segregated samples to UV light led to cross-linking of the DiynePC-rich domains into solid filter matrices; the nonpolymerizable DOPC-rich phase regions were transformed to void regions in the filters. We varied the DiynePC/DOPC molar ratio from 60/40 to 80/20 to adjust the cutoff size of the filter barrier and used two model membrane-embedded species with different sizes to examine the filtering capability. Our results demonstrated that the filter barrier constructed by the phase segregation method could be used to distinguish between the size of TR (the membrane-embedded area is similar to the size of a regular phospholipid) and the size of CT complex (the membrane-embedded area is several times larger than the size of TR). When the DiynePC/DOPC molar ratio was 60/40, both species showed high penetration ratios. However, when the ratio was increased to 70/30, only the smaller (TR) species showed a relatively high penetration ratio. When the ratio was increased to 80/20, neither TR nor CT complex could penetrate the filter region. The results demonstrated that the phase segregation method could be used to construct filters in the SLB and that the molar ratio of polymerizable lipids to nonpolymerizable lipids could be used to adjust the filter cutoff size.

ACKNOWLEDGMENTS

We would like to thank the National Science Council of Taiwan (NSC 102-2221-E-002-153-MY3) and the Career Development Grant from National Taiwan University for financial support.

¹A. C. Neville, *Biology of Fibrous Composites: Development Beyond the Cell Membrane*/A.C. Neville (Cambridge University Press, New York, NY, USA, 1993).

²L. Rajendran and K. Simons, *J. Cell Sci.* **118**(6), 1099–1102 (2005).

³R. R. Sprenger and J. G. Horrevoets, *Proteomics* **7**, 2895–2903 (2007).

⁴Y. Z. Zheng and L. J. Foster, *Proteomics* **72**, 12–22 (2009).

⁵E. T. Castellana and P. S. Cremer, *Surf. Sci. Rep.* **61**(10), 429–444 (2006).

⁶L. Chao and S. Daniel, *J. Am. Chem. Soc.* **133**(39), 15635–15643 (2011).

⁷L. Chao, A. P. Gast, T. A. Hatton, and K. F. Jensen, *Langmuir* **26**(1), 344–356 (2010).

⁸C. Steinem, A. Janshoff, W.-P. Ulrich, M. Sieber, and H.-J. Galla, *Biochim. Biophys. Acta* **1279**(2), 169–180 (1996).

⁹L. K. Nielsen, A. Vishnyakov, K. Jørgensen, T. Bjørnholm, and O. G. Mouritsen, *J. Phys.: Condens. Matter* **12**(8A), A309–A314 (2000).

¹⁰V. Kiessling and L. K. Tamm, *Biophys. J.* **84**(1), 408–418 (2003).

¹¹L. K. Tamm, *Biochemistry* **27**(5), 1450–1457 (1988).

¹²C. Dietrich, R. Merkel, and R. Tampe, *Biophys. J.* **72**(4), 1701–1710 (1997).

- ¹³S. Daniel, A. J. Diaz, K. M. Martinez, B. J. Bench, F. Albertorio, and P. S. Cremer, *J. Am. Chem. Soc.* **129**(26), 8072–8073 (2007).
- ¹⁴C. Liu, C. F. Monson, T. Yang, H. Pace, and P. S. Cremer, *Anal. Chem.* **83**(20), 7876–7880 (2011).
- ¹⁵P. Jönsson, J. P. Beech, J. O. Tegenfeldt, and F. Höök, *J. Am. Chem. Soc.* **131**(14), 5294–5297 (2009).
- ¹⁶J. Neumann, M. Hennig, A. Wixforth, S. Manus, J. O. Radler, and M. F. Schneider, *Nano Lett.* **10**(8), 2903–2908 (2010).
- ¹⁷H. Shu-Kai, H. Sheng-Wen, M. Hsun-Yen, C. Ya-Ming, C. Yung, and C. Ling, *Sci. Technol. Adv. Mater.* **14**(4), 044408 (2013).
- ¹⁸E. J. Henley, J. D. Seader, and D. K. Roper, *Separation Process Principles* (Wiley, Hoboken, NJ, 2011).
- ¹⁹T. Okazaki, Y. Tatsu, and K. Morigaki, *Langmuir* **26**(6), 4126–4129 (2010).
- ²⁰K. Morigaki, K. Kiyosue, and T. Taguchi, *Langmuir* **20**(18), 7729–7735 (2004).
- ²¹S. May, *Soft Matter* **5**(17), 3148–3156 (2009).
- ²²D. Kashchiev, *Nucleation: Basic Theory with Applications* (Butterworth-Heinemann, 2000).
- ²³N. Otsu, *IEEE Transactions on Systems, Man and Cybernetics* **9**(1), 62–66 (1979).
- ²⁴A. Yavlovich, A. Singh, S. Tarasov, J. Capala, R. Blumenthal, and A. Puri, *J. Therm. Anal. Calorim.* **98**(1), 97–104 (2009).
- ²⁵A. Puri and R. Blumenthal, *Acc. Chem. Res.* **44**(10), 1071–1079 (2011).
- ²⁶P. Jönsson, J. P. Beech, J. O. Tegenfeldt, and F. Höök, *Langmuir* **25**(11), 6279–6286 (2009).
- ²⁷J. M. Smaby, M. M. Momsen, H. L. Brockman, and R. E. Brown, *Biophys. J.* **73**(3), 1492–1505 (1997).
- ²⁸C. E. Miller, J. Majewski, R. Faller, S. Satija, and T. L. Kuhl, *Biophys. J.* **86**(6), 3700–3708 (2004).
- ²⁹See supplementary material at <http://dx.doi.org/10.1063/1.4895570> for pure DOPC control experiments.
- ³⁰A. G. Peter Jönsson and Fredrik Höök, *Anal. Chem.* **83**(2), 604–611 (2011).
- ³¹C.-Y. Lin and L. Chao, *Langmuir* **29**(42), 13008–13017 (2013).
- ³²K. Tawa and K. Morigaki, *Colloids Surf. B* **81**(2), 447–451 (2010).